

Melting studies of short DNA hairpins containing the universal base 5-nitroindole

Peter M. Vallone and Albert S. Benight*

Department of Chemistry, 845 West Taylor Street, Room 4500, University of Illinois at Chicago, Chicago, IL 60607, USA

Received March 31, 1999; Revised and Accepted July 2, 1999

ABSTRACT

Effects of the universal base 5-nitroindole on the thermodynamic stability of DNA hairpins having a 6 bp stem and four base loops were investigated by optical absorbance and differential scanning calorimetry techniques. Melting studies were conducted in buffer containing 115 mM Na⁺. Five different modified versions of DNA hairpins containing a 5-nitroindole base or bases substituted at different positions in the stem and loop regions were examined. Thermodynamic parameters of the melting transitions estimated from a two-state analysis of optical melting curves and measured directly by calorimetry revealed that the presence of 5-nitroindole bases in the duplex stem or loop regions of short DNA hairpins significantly affects both their enthalpic and entropic melting components in a compensating manner, while the transition free energy varies linearly with the transition temperature. The calorimetrically determined enthalpy and entropy values of the modified hairpins were considerably smaller (43–53%) than the two-state optical parameters, suggesting that solvent effects may be significant in the melting processes of these hairpins. Results of circular dichroism measurements also revealed slight differences between the modified hairpins and the control in both the duplex and melted states, suggesting subtle structural differences between the control and DNA hairpins containing a 5-nitroindole base or bases.

INTRODUCTION

Emerging applications of DNA hybridization-based technologies, coupled with the ever increasing desire to finely tune hybridization reactions, has spurred efforts directed toward constructing a synthetic universal DNA base analog. Among other things, when incorporated into a duplex the ideal universal DNA base should be able to form stable base pairs with the four natural bases and be capable of priming DNA synthesis by DNA polymerases. It is desired that such a universal base would base pair non-discriminately when incorporated into a DNA duplex and not significantly perturb duplex structure. A base that could behave in this manner would be expected to maximize

stacking while minimizing hydrogen bonding interactions, without altering stability of the double-stranded structure. In addition, the nucleotide triphosphate of the universal base should function like a natural base *in vivo* and therefore be able to be cloned (1). Several examples of base analogs that could have these desirable characteristics have been reported (2–6). One of these, the universal base 5-nitroindole (5-NI), was the subject of the studies reported here.

Nucleoside synthesis of 5-NI was first described in 1994 by Loakes and Brown, who reported the complete synthesis of 4, 5 and 6-nitroindole (3). The effect on duplex stability of incorporating these base analogs was determined from melting analysis of a series of 17 bp duplex DNAs containing one or more universal base moieties substituted at varying positions for natural DNA bases. Their studies concluded that all three universal bases destabilized the duplexes, and 5-NI was the least destabilizing.

In this paper we report results of optical and calorimetric melting studies of DNA hairpins containing a 5-NI base or bases at different positions in the stem and loop regions. The hairpins were designed to form from 16 base self-complementary single-stranded oligomers that fold intramolecularly to DNA hairpins with 6 bp in the stem and four bases in the loop. Results for the hairpins containing 5-NI are compared directly with results of melting analysis of a natural DNA hairpin with a 6 bp duplex stem and T₄ loop that was characterized by optical and calorimetric melting techniques as part of a previous study (7).

MATERIALS AND METHODS

DNA samples

Six partially self-complementary DNA strands were prepared. Five of these contained the universal base 5-NI at one or more different positions in the strands. The self-complementary sequences were chosen to encourage formation of intramolecular DNA hairpins. DNA strands were synthesized on an Applied Biosystems ABI380B automated DNA synthesizer. The 5-NI base was purchased from Glen Research (Arlington, VA) as a trityl protected phosphoramidite, rehydrated in dry acetonitrile, placed on the DNA synthesizer and used fresh within 24 h. Single-stranded oligomers were purified by denaturing gel electrophoresis and exchanged via dialysis into melting buffer. The structure of 5-NI as a nucleoside is shown in Figure 1.

*To whom correspondence should be addressed. Tel: +1 312 996 0774; Fax: +1 312 996 0431; Email: abenight@uic.edu

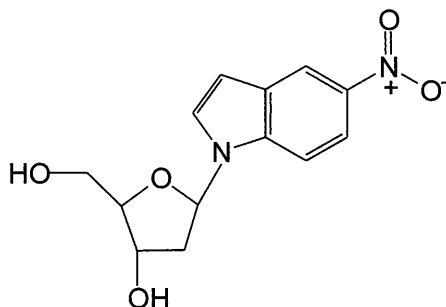


Figure 1. Structure of the 5-nitroindole DNA nucleoside.

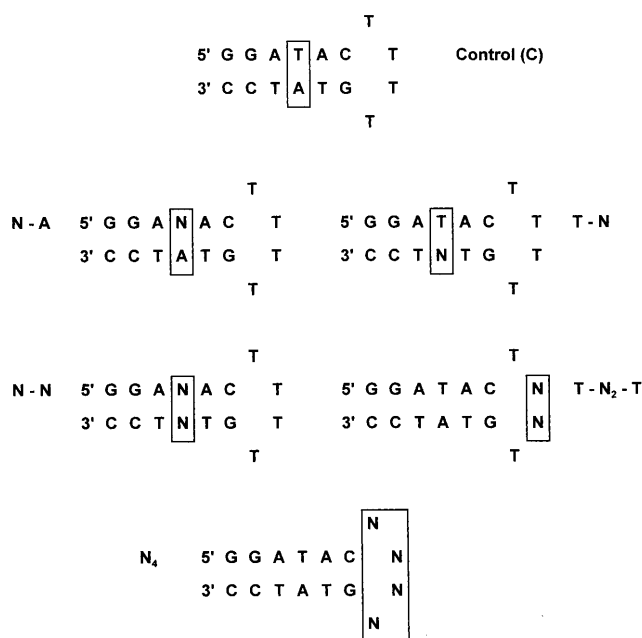


Figure 2. DNA molecules of this study. Five modified hairpins having a 5-nitroindole base (N) in the stem and loop regions were prepared and studied. Results for the modified hairpins were compared to those for the natural DNA control (C). The nomenclature used for referring to each hairpin throughout the text is given.

Sequences of the six DNAs studied are depicted in Figure 2 in their presumed hairpin configuration. Position of the 5-NI base in these molecules is designated by an N. The nomenclature used to refer to each hairpin is also given in Figure 2. The control, hairpin C, is the natural sequence with 6 bp in the stem and a T₄ single-stranded loop and does not contain a 5-NI base. Results for C serve as the basis for comparisons of the relative melting properties of the other molecules having 5-NI bases. Hairpins containing a single 5-NI base opposing either an A or T residue on the 5' or 3' side of the stem are designated N-A and T-N, respectively. The molecule having a pair of opposing 5-NI bases is designated N-N. Hairpins designated N₄ and T-N₂-T

have a loop comprised of four 5-NI bases or two 5-NI bases flanked by T residues, respectively.

Optical melting experiments

Melting buffer comprised 100 mM sodium chloride, 10 mM sodium phosphate and 1 mM EDTA, pH 7.5. Optical melting curves were collected as the UV absorbance at 268 nm versus temperature. Melting data were acquired with a Hewlett Packard 8452 diode array single beam spectrophotometer equipped with a thermostated temperature controller and sample holder. For all hairpin samples, melting experiments were performed over the strand concentration range 0.8–40 μM. DNA concentrations were determined from extinction coefficients calculated using the published nearest neighbor nucleotide values at 260 nm (8). The extinction coefficient for 5-NI was reported to be $\epsilon = 18\,300\text{ M/cm}$ at $\lambda_{\text{max}} = 266\text{ nm}$ for the free base, not the nucleotide or nucleoside (1). The reported extinction coefficient for the nucleoside derivative is slightly lower at $\epsilon = 16\,000\text{ M/cm}$, $\lambda_{\text{max}} = 260\text{ nm}$ (R.L.Somers, personal communication). We assumed that the 5-NI nucleoside has spectral properties very similar to adenosine with $\epsilon = 15\,400\text{ M/cm}$ at $\lambda_{\text{max}} = 259\text{ nm}$, which is only slightly lower than the reported value for the 5-NI nucleoside. Thus, in calculations of the extinction coefficients using the nearest neighbor values at 260 nm, a 5-NI base was treated as an adenine. Prior to melting, samples were first heated to 95°C for 15 min, then incubated on ice for 15 min. Samples were degassed by bubbling with a fine stream of helium for at least 30 min. Degassed samples were gently filtered through a 0.45 μm nylon filter into a dry quartz cuvette. Depending on the sample concentration, cuvette path lengths were 0.1 or 1 cm. Absorbance values at 268 nm versus temperature were collected over the range 12–85°C. Samples were allowed to equilibrate for 15 min at the beginning temperature of each heating-cooling cycle. Temperature was increased (and decreased) linearly at a rate of ~35°C/h while the absorbance at 268 nm was continuously monitored. For each sample, at least three complete (heating-cooling) transition curves were collected at each DNA concentration.

Prior to melting experiments on each sample, a buffer baseline was acquired by simply increasing the temperature of the buffer alone under conditions identical to those for melting the DNAs. The buffer baseline was subtracted from the raw absorbance versus temperature curves for each DNA sample to yield baseline corrected absorbance versus temperature curves for the samples alone. Procedures for reduction of these data to provide curves of the net fraction of broken base pairs, $\theta_B(T)$, versus temperature and to obtain derivative curves, $d\theta_B/dT$, versus temperature have been described (9).

Melting curve parameters employed to evaluate transition thermodynamic parameters were the peak height maximum $(d\theta_B/dT)_{\text{max}}$ and the transition temperature T_m , defined as the temperature at $(d\theta_B/dT)_{\text{max}}$. The following are the familiar expressions that use these graphically determined parameters to estimate the melting van't Hoff thermodynamics assuming a two-state melting transition (10).

$$\Delta H_{\text{vH}} = 4RT_m^2 (d\theta_B/dT)_{\text{max}} \quad 1$$

$$\Delta S_{\text{vH}} = \Delta H_{\text{vH}}/T_m \quad 2$$

Obviously, in this analysis the transition enthalpy and entropy are linked directly through T_m .

Calorimetric melting experiments

Excess heat capacities of DNA hairpin samples, ΔC_p^{ex} , as a function of temperature were measured on a Microcal MC-2 ultrasensitive differential scanning calorimeter (DSC) instrument (Northampton, MA). The instrument was calibrated with a standard known electrical pulse prior to data collection. To prepare them for DSC melting experiments, DNAs were dialyzed exhaustively against melting buffer. Sample quantity was ~ 25 OD/ml (or greater) in a total volume of ~ 2 ml. This amounted to strand concentrations ≥ 150 μM . Thus, DSC melting curves were collected at DNA strand concentrations 4–187 times higher than optical melting curves. At least 10 buffer versus buffer baselines (reference and sample cell both containing melting buffer only) were scanned prior to acquisition of actual DNA versus buffer curves. For DNA samples, 8 to 10 scans were collected from 4 to 100°C at a heating rate of $60^\circ\text{C}/\text{h}$. When acquisition of DSC melting curves on a particular sample was complete the sample and reference cells of the calorimeter were thoroughly cleaned by washing with diluted, warm standard detergent solution and rinsing exhaustively with nanopure water. The procedure was then repeated for the next melting curve measurement, starting with the buffer versus buffer scans followed by melting of the next DNA sample. The DSC transition temperature, $T_{\text{m Cal}}$, was determined as the temperature at the peak height maximum on the baseline corrected ΔC_p^{ex} versus temperature curve. The integrated area under the concentration corrected curve provided the reported DSC transition enthalpy,

$$\int \Delta C_p^{\text{ex}} dT = \Delta H_{\text{Cal}} \quad 3$$

The DSC transition entropy values were determined from the integrated area under curves of $\Delta C_p^{\text{ex}}/T$ versus temperature,

$$\int (\Delta C_p^{\text{ex}}/T) dT = \Delta S_{\text{Cal}} \quad 4$$

For the molecules of this study it was found that $\Delta S_{\text{Cal}} = \Delta H_{\text{Cal}}/T_{\text{m}}$ within the experimental errors for T_{m} and ΔH_{Cal} . Additional significant figures were included in values for ΔH_{Cal} (and ΔH_{vH}) and ΔS_{Cal} (and ΔS_{vH}) to allow for a more accurate calculation of ΔG_{Cal} (and ΔG_{vH}). Values of the thermodynamic transition parameters were also determined by fitting DSC melting curves with a two-state-model.

Circular dichroism (CD)

CD spectra were collected on a Jasco J-600 spectropolarimeter at temperatures controlled by a thermostated sample cell holder and circulating water bath. Temperature of the sample holder was maintained at 10 or 80°C . Sample requirements for CD measurements were similar to those for absorbance measurements. DNA solutions having OD readings between ~ 0.4 and 0.8 were optimal. Three milliliter sample solutions were placed in a 1.0 cm path length cell. Samples were allowed to equilibrate in the sample holder at the desired temperature for at least 15 min prior to collection of CD spectra. Data were collected from 320 to 200 nm at a rate of 10 nm/min and wavelength increment of 0.4 nm. To avoid absorbance interference at short wavelengths (≤ 235 nm), CD spectra were collected on DNA samples in melting buffer that did not contain EDTA.

CD spectra are presented as plots of $\Delta \epsilon_{\text{L-R}}$ (per cm/M) versus wavelength (nm). At least five scans were collected for each sample at 10 and 80°C . The average of these scans at each

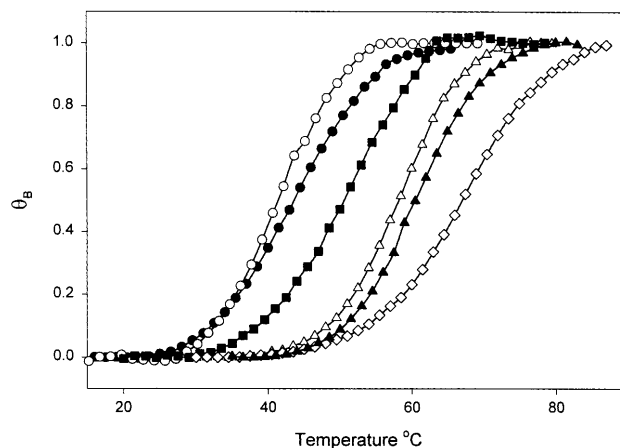


Figure 3. Normalized optical melting curves of the DNA hairpins. Plots of the fraction of broken base pairs, θ_B , versus temperature for the six DNA hairpins of Figure 2. These are the average of at least three melting experiments. According to the nomenclature assigned for the hairpin molecules in Figure 2, symbols for the melting curves are as follows: N_4 , open diamonds; T- N_2 -T, filled triangles; C, open triangles; N-N, filled squares; N-A, filled circles; T-N, open circles. The optical transition temperature, $T_{\text{m Opt}}$, derived from these curves is summarized for each hairpin in Table 1.

temperature was normalized for total strand concentration and used in further analysis.

The fundamental underlying spectral features of the CD spectra collected for the DNA molecules were deconvoluted using singular value decomposition (SVD). This technique has been applied in a number of contexts, most notably in the analysis of CD spectral data from DNA and proteins. For our application of the method, the CD spectrum collected from 320 to 212 nm at 10 and 80°C for each DNA molecule was cast as a row vector comprised of $(320 - 212)/0.4 \approx 270$ elements. The set of vectors for the six DNA molecules at 10 and 80°C were subjected to SVD analysis. The analytical procedure was essentially that described previously (11).

SVD analysis determines the minimum number of basis spectra with significant weight that can be linearly combined to produce each measured CD spectrum within certain limits. For each molecule the set of linear coefficients for the basis vectors at 10 and 80°C were determined. Comparison of the values of these coefficients revealed subtle differences between the CD spectra of the molecules containing 5-NI and the control molecule, in the duplex (10°C) and melted (80°C) states.

RESULTS

Optical melting curves experiments

Optical melting curves for the molecules of Figure 2 are shown in Figure 3, where the fraction of broken base pairs, θ_B , is plotted versus temperature. The curves in Figure 3 were derived from plots of the absorbance at 268 nm versus temperature, collected (but not shown) for each DNA in buffered 115 mM Na^+ solvent. All DNAs examined exhibited melting temperatures independent of strand concentration from 0.8 to 40.0 μM . This is consistent

Table 1. Transition temperatures determined from optical ($T_{m\text{Opt}}$) and DSC ($T_{m\text{Cal}}$) melting curves for the six hairpins of this study

Molecule ^a	% A	$T_{m\text{Opt}}$ (°C)	$T_{m\text{Cal}}$ (°C)	$\Delta T_{m\text{Opt}}$ (°C)	$\Delta T_{m\text{Cal}}$ (°C)
Control	16.3 ± 0.6	59.4 ± 0.2	59.3 ± 0.3	0.0	0.0
N-A	10.8 ± 1.1	42.3 ± 0.4	41.8 ± 0.5	-17.1 ± 0.4	-17.5 ± 0.6
T-N	10.7 ± 1.0	40.9 ± 0.4	40.5 ± 0.4	-18.5 ± 0.4	-18.8 ± 0.5
N-N	11.7 ± 0.8	52.5 ± 0.2	49.1 ± 0.4	-6.9 ± 0.3	-10.2 ± 0.5
T-N ₂ -T	14.5 ± 0.7	60.3 ± 0.2	63.1 ± 0.3	0.9 ± 0.3	3.8 ± 0.0
N ₄	13.5 ± 0.7	65.7 ± 0.2	69.3 ± 0.4	6.3 ± 0.3	10.0 ± 0.5

^aDNA hairpins depicted in Figure 2.

Also shown are the differences, $\Delta T_{m\text{Cal}}$ and $\Delta T_{m\text{Opt}}$, between the DSC and optical transition temperatures of the control hairpin and modified hairpins containing the 5-NI base or bases. The relative hyperchromicity changes at 268 nm for melting of the hairpins are shown in the first column.

Table 2. Thermodynamic transition parameters determined from a two-state van't Hoff analysis of optical melting curves (ΔH_{vH} , ΔS_{vH} and $\Delta G_{293\text{vH}}$) and measured directly from DSC melting curves (ΔH_{Cal} , ΔS_{Cal} and $\Delta G_{293\text{Cal}}$)

Molecule ^{a,b}	ΔH_{vH} (kcal/mol)	ΔH_{Cal} (kcal/mol)	ΔS_{vH} (eu)	ΔS_{Cal} (eu)	$\Delta G_{293\text{vH}}$ (kcal/mol)	$\Delta G_{293\text{Cal}}$ (kcal/mol)
Control	-47.2	-41.1	-142.0	-129.5	-5.6	-3.2
N-A	-28.9	-19.5	-91.5	-61.8	-2.0	-1.3
T-N	-36.7	-18.3	-116.7	-58.6	-2.4	-1.2
N-N	-33.9	-16.0	-104.1	-49.7	-3.4	-1.4
T-N ₂ -T	-43.5	-28.0	-130.4	-83.5	-5.3	-3.5
N ₄	-42.9	-29.2	-126.7	-85.3	-5.8	-4.2

^aDNA hairpins depicted in Figure 2.

^bEstimated uncertainty on the ΔH_{vH} and ΔS_{vH} values is ±5%. Uncertainty in ΔG_{vH} values is ±0.5 kcal/mol.

with our assumption that the strands reside primarily in the hairpin state under the conditions of the optical melting experiments. The $T_{m\text{Opt}}$ values for the molecules, determined from the temperature at peak height maximum on their derivative melting curves (not shown), are summarized in Table 1. These values and the melting curves in Figure 3 reveal the most stable hairpins to be N₄ (open diamonds, $T_{m\text{Opt}} = 65.7^\circ\text{C}$) and T-N₂-T (filled triangles, $T_{m\text{Opt}} = 60.3^\circ\text{C}$) that have 5-NI bases in the loop. The hairpins with 5-NI in the stem are less stable than C, in the descending order C (open triangles, $T_{m\text{Opt}} = 59.4^\circ\text{C}$) > N-N (filled squares, $T_{m\text{Opt}} = 52.5^\circ\text{C}$) > N-A (filled circles, $T_{m\text{Opt}} = 42.3^\circ\text{C}$) > T-N (open circles, $T_{m\text{Opt}} = 40.9^\circ\text{C}$). Also given in Table 1 are $\Delta T_{m\text{Opt}}$ values, the result of subtracting $T_{m\text{Opt}}$ of hairpin C from $T_{m\text{Opt}}$ of each of the modified hairpins containing a 5-NI base (or bases). As seen from the $\Delta T_{m\text{Opt}}$ values in Table 1, a single 5-NI base in the stem causes the largest relative change in stability. Hairpins N-A and T-N have T_m values ~17.5°C lower than hairpin C. When two 5-NI bases oppose each other, as in hairpin N-N, the hairpin is considerably more stable than those having a single 5-NI base in the stem, but still less stable than hairpin C by 7°C. Interestingly, the hairpins with the 5-NI bases in the loops display relatively higher stabilities than C. Hairpin T-N₂-T is only slightly more stable ($\Delta T_{m\text{Opt}} = 0.9^\circ\text{C}$)

while hairpin N₄ is significantly more stable ($\Delta T_{m\text{Opt}} = 6.3^\circ\text{C}$). This higher stability could be due to several factors, including the presence of more favorable stacking interactions between the 5-NI bases in the loops and interactions with the surrounding solvent, not present in the T₄ loop of the control.

The relative hyperchromicity changes for each hairpin are also shown in Table 1. These increases in the absorbance at 268 nm upon melting range from 16.3% for the control hairpin to ~11% for hairpins N-A, T-N and N-N. For hairpins N₄ and T-N₂-T, with 5-NI bases in their loops, the absorbance changes upon melting are ~14%. Relatively lower hyperchromicity changes for melting the modified hairpins compared to the control suggest, when in the hairpin stems and to a lesser extent when in the loops, the 5-NI bases act to increase the absorbance of the fully intact hairpins and/or decrease absorbance of their melted single strands relative to the intact duplex and melted states of the control hairpin.

The van't Hoff parameters, ΔH_{vH} , ΔS_{vH} and ΔG_{vH} , evaluated from graphical analysis of melting curves assuming a two-state melting process, are summarized in Table 2. Estimated uncertainty on the ΔH_{vH} and ΔS_{vH} values is ±5%. Uncertainty in ΔG_{vH} values is ±0.5 kcal/mol. Table 2 reveals that ΔH_{vH} and ΔS_{vH} for the modified hairpins are smaller than for the control

Table 3. Differences, $\Delta\Delta H$, $\Delta\Delta S$ and $\Delta\Delta G_{293}$, between the optical and DSC thermodynamic parameters of the control and the five modified hairpins

Molecule ^a	$\Delta\Delta H_{\text{vH}}$ (kcal/mol)	$\Delta\Delta H_{\text{Cal}}$ (kcal/mol)	$\Delta\Delta S_{\text{vH}}$ (eu)	$\Delta\Delta S_{\text{Cal}}$ (eu)	$\Delta\Delta G_{293 \text{ vH}}$ (kcal/mol)	$\Delta\Delta G_{293 \text{ Cal}}$ (kcal/mol)
Control	0.0	0.0	0.0	0.0	0.0	0.0
N-A	18.3	21.6	50.5	67.7	3.6	1.9
T-N	10.5	22.8	25.3	70.9	3.2	2.0
N-N	13.3	25.1	37.9	79.8	2.2	1.8
T-N ₂ -T	3.7	13.1	11.6	46.0	0.3	-0.3
N ₄	4.3	11.9	15.3	44.2	-0.2	-1.0

^aDNA hairpins depicted in Figure 2.

hairpin. Perhaps more informative for relative comparisons are the differences between ΔH_{vH} and ΔS_{vH} for the modified and control hairpins, summarized in Table 3 as the values of $\Delta\Delta H_{\text{vH}}$ and $\Delta\Delta S_{\text{vH}}$. For modified hairpins with a 5-NI base or bases in the stem, $\Delta\Delta H_{\text{vH}}$ ranges from 10.5 to 18.3 kcal/mol. Likewise, for these hairpins $\Delta\Delta S_{\text{vH}}$ is from 25 to 50 cal/mol K. Even though there are fairly large differences between the ΔH_{vH} and ΔS_{vH} values of modified hairpins and the control, differences in the free energies, $\Delta\Delta G_{\text{vH}}$, are relatively small and range from 2.2 to 3.6 kcal/mol for the modified hairpins with the 5-NI bases in their stems. Hairpins containing 5-NI in the stem had ΔG_{vH} values smaller than the control, consistent with the trend seen for the $T_{\text{m Opt}}$ values. For the hairpins with the 5-NI bases in the loops, which actually had $T_{\text{m Opt}}$ values higher than the control, $\Delta\Delta H_{\text{vH}}$ and $\Delta\Delta S_{\text{vH}}$ are smaller than for the hairpins with the 5-NI bases in the stem, but still positive, i.e. both ΔH_{vH} and ΔS_{vH} for these hairpins are smaller than the control. However, their ΔH_{vH} and ΔS_{vH} values combine to make $\Delta\Delta G_{\text{vH}}$ values for the hairpins that are close to, or only slightly less than 0. Results of this optical melting analysis suggest that the 5-NI base affects both enthalpic and entropic components of hairpin melting in a compensating manner such that ΔG_{vH} remains linearly related to $T_{\text{m Opt}}$.

Results of the analysis of optical melting curves are founded upon the assumption that the melting transitions of the hairpins are two-state. Thermodynamic parameters evaluated from the graphical two-state analysis depend heavily on the curve shapes of optical melting curves, because of the direct influence of $(d\theta_{\text{B}}/dT)_{\text{max}}$ on the van't Hoff enthalpy, $\Delta H_{\text{vH}} = 4RT_{\text{m}}^2(d\theta_{\text{B}}/dT)_{\text{max}}$. Although N₄ and T-N₂-T displayed higher $T_{\text{m Opt}}$ values than C, the peak heights were both slightly lower than for C. The result is overall lower ΔH_{vH} values. This is probably because the melting behavior of hairpins containing the 5-NI base or bases deviates from two-state behavior. Such departure from two-state melting could very well manifest as lower peak heights on differential melting curves. In order to evaluate thermodynamic parameters without relying on the two-state model assumption, model-independent thermodynamics for the hairpins were measured directly by DSC. Results of these experiments are described next.

Melting by differential scanning microcalorimetry

DSC melting experiments provided a model-independent measurement of transition thermodynamic parameters of the DNA hairpins containing the 5-NI base or bases. Three typical

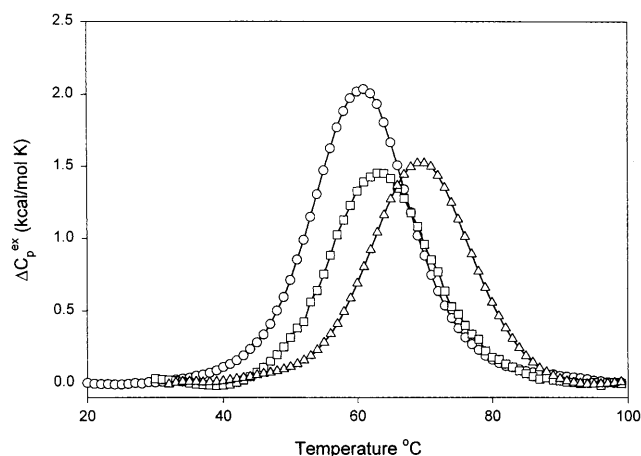


Figure 4. Melting curves from DSC. Three DSC melting curves are shown as plots of excess heat capacity ΔC_p^{ex} versus temperature. The curves shown are for hairpins C (open circles), T-N₂-T (open squares) and N₄ (open triangles). The DSC transition temperatures, $T_{\text{m Cal}}$, values determined for all molecules are given in Table 1.

DSC melting curves are shown in Figure 4 as plots of excess heat capacity ΔC_p^{ex} versus temperature. The curves shown are for hairpins C (open circles), T-N₂-T (open squares) and N₄ (open triangles). The DSC transition temperature, $T_{\text{m Cal}}$, values are given in Table 1. As can be seen, only for the control and hairpins N-A and T-N with one 5-NI base in the stem are the values of $T_{\text{m Cal}}$ and $T_{\text{m Opt}}$ in agreement within the experimental errors. For hairpin N-N, $T_{\text{m Cal}}$ is 3.4°C lower than $T_{\text{m Opt}}$. For hairpins T-N₂-T and N₄, $T_{\text{m Cal}}$ values are 2.8 and 3.4°C higher, respectively, than the corresponding $T_{\text{m Opt}}$ values.

As mentioned earlier and discussed later, these higher $T_{\text{m Cal}}$ values were obtained on DNA samples at concentrations 4–187 times higher than in the optical experiments. The observed higher $T_{\text{m Cal}}$ values could reveal the presence of additional molecular species such as the bulged duplex or a small amount of intermolecular association between these molecules at the higher concentrations at which DSC experiments were run. In addition, solvent effects associated with the hydrophobic 5-NI base or bases could also contribute to observed differences between the values of $T_{\text{m Cal}}$ and $T_{\text{m Opt}}$. Although there is no

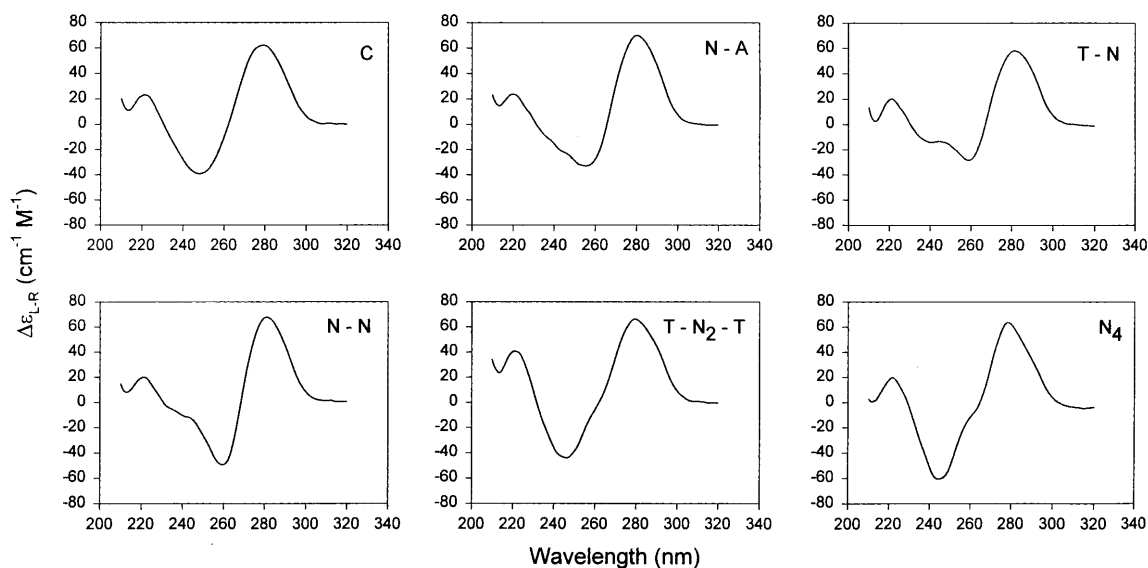


Figure 5. The CD spectra, plots of the ellipticity difference $\Delta\epsilon_{L,R}$ (per cm/M) versus wavelength (nm) collected at 10°C, for the six hairpins of Figure 2. The spectra correspond to the hairpins according to the nomenclature of Figure 2. These spectra are the average of at least five scans normalized for total strand concentration.

quantitative agreement between $T_{m,Cal}$ and $T_{m,Opt}$ for all hairpins, the same trend is seen in the $\Delta T_{m,Cal}$ values, which are the differences between the $T_{m,Cal}$ of the modified hairpins and the control. As the right columns of Table 1 indicate, the values of $\Delta T_{m,Cal}$ and $\Delta T_{m,Opt}$ display the same trends in stability for the hairpins, but are not in quantitative agreement in all cases.

The thermodynamic parameters, ΔH_{Cal} , ΔS_{Cal} and ΔG_{Cal} , obtained from DSC melting experiments are given in Table 2. Like the optical values, estimated uncertainties in ΔH_{Cal} and ΔS_{Cal} are $\pm 5\%$. Uncertainty in ΔG_{Cal} values is ± 0.5 kcal/mol. As found for the optical parameters, Table 2 reveals that ΔH_{Cal} and ΔS_{Cal} for the modified hairpins are smaller than the control hairpin. Differences between ΔH_{Cal} and ΔS_{Cal} for the modified hairpins and the control are summarized in the $\Delta\Delta H_{Cal}$ and $\Delta\Delta S_{Cal}$ values in Table 3. The magnitudes of the differences are greater for the DSC than the optical parameters, but the relative order for the hairpins is the same. For modified hairpins with a 5-NI base or bases in the stem, $\Delta\Delta H_{Cal}$ ranges from 21.6 to 25.1 kcal/mol. Likewise, for these hairpins $\Delta\Delta S_{Cal}$ is from 68 to 80 cal/mol K. Even though there are fairly large differences between the ΔH_{Cal} and ΔS_{Cal} values of the modified hairpins and the control, differences in their free energies are relatively smaller and $\Delta\Delta G_{Cal}$ is ~ 2.0 kcal/mol for the modified hairpins with the 5-NI bases in their stems. Hairpins containing 5-NI in the stem had ΔG_{Cal} values smaller than the control, consistent with the trend seen for the $T_{m,Cal}$ values. For the hairpins with the 5-NI bases in the loops, which actually had $T_{m,Cal}$ values higher than the control, $\Delta\Delta H_{Cal}$ and $\Delta\Delta S_{Cal}$ values are smaller than for the hairpins with the 5-NI bases in the stems, but still positive, i.e. both ΔH_{Cal} and ΔS_{Cal} for these hairpins are smaller than the control. However, their $\Delta\Delta H_{Cal}$ and $\Delta\Delta S_{Cal}$ values combine to make $\Delta\Delta G_{Cal}$ values for the hairpins that are less than 0. The DSC melting analysis also indicates that the 5-NI bases affect both enthalpic and entropic components of hairpin melting in a compensating manner. As found for the optical experiments,

ΔG_{Cal} is linearly related to $T_{m,Cal}$. Thermodynamic parameters obtained by fitting the DSC curves to a two-state model (not shown) were slightly greater (9–20%) than the DSC values reported in Table 2. No appreciable difference in the ΔC_p^{ex} values before and after the transitions could be detected on the DSC melting curves collected for the six hairpins of this study.

Although they are quantitatively different, the DSC and optical data are in qualitative agreement, i.e. both techniques find the same relative ranking of the thermodynamic parameters for the 5-NI-modified hairpins compared to the control. Most importantly, the DSC measurements confirm that hairpins with 5-NI bases in the loop region are more stable than the control hairpin with a T_4 loop. The large differences between the optical and DSC thermodynamic parameters suggests additional features of the melting transitions of the hairpins containing a 5-NI base or bases may contribute to the DSC measurements that are not detected in optical melting experiments.

Results from CD measurements

The CD spectra, plots of $\Delta\epsilon_{L,R}$ versus wavelength collected at 10°C for the six hairpins shown in Figure 1, are displayed in Figure 5. Initial inspection of the CD spectra does not reveal a great deal of difference between them. All six molecules exhibit typical B-like spectra with a positive band at ~ 275 nm, crossover from positive to negative ellipticity at ~ 258 nm and a negative band at ~ 240 nm (12). The spectra for hairpins N-N and T-N appear to be the most different from that of C. A more in-depth analysis of the spectra by SVD revealed more clearly the existence of subtle differences in the spectra. Analysis by SVD of the CD spectra collected at 10 and 80°C for the six hairpins revealed that their collected spectra can be generated from three subspectra (not shown). At 10°C the relative weights of the subspectra were 0.93, 0.05 and 0.01. At 80°C the relative weights were 0.94, 0.04 and 0.02. When combined with their appropriate linear coefficients and added together

these subspectra produce each measured spectrum to >99%. Similarity of the CD spectra for each hairpin containing a 5-NI base or bases and the control in the duplex (10°C) and melted (80°C) states was assessed by the degree of correlation between the three linear coefficients for the subspectra obtained from SVD analysis for each modified hairpin and those found for the control at these temperatures. Results are shown in Table 4, where correlation coefficients (r^2 values) obtained for each modified hairpin compared to C are summarized. Essentially, this comparison reveals how well the spectra of each modified hairpin agree with those of the control at the two temperatures, e.g. for perfect agreement $r^2 = 1.0$. The order of the correlation coefficients for the CD spectra collected at 10°C (where the hairpins are maximally intact) is C (1.0) > T-N₂-T (0.98) > N-A (0.96) > N₄ (0.95) > T-N (0.90) > N-N (0.85). The same analysis of the CD spectra collected at 80°C (presumably where the hairpins are melted) yields a slightly different order for the correlation coefficients, C (1.0) > T-N (0.95) > N₄ (0.94) = N-A > T-N₂-T (0.92) > N-N (0.81). Thus, this analysis indicates that hairpins N₄, T-N, N-T₂-N and N-A in the duplex form at 10°C have CD spectra most like that of C. At 80°C the r^2 values for hairpins T-N (0.95) and T-N₂-T (0.92) interchange in relative order with respect to C. The CD spectra for hairpin N-N differ the most from the spectra of C at 10 and 80°C. If the CD spectrum can be taken to represent a measure of the structural features of the hairpins in the duplex and melted states, then the above results suggest that, although hairpins containing 5-NI adopt structures very similar to the control, the 5-NI base or bases in the stem may induce subtle perturbations of the duplex stem structure. The analysis also suggests that subtle differences may exist in the single strand states of the 5-NI and control hairpins. This is consistent with our interpretations of the differences between the optical and DSC thermodynamic parameters.

Table 4. Correlation coefficients (r^2 values) obtained for the modified hairpins containing a 5-NI base or bases compared to the control

Molecule ^a	10°C	80°C
Control	1.00	1.00
N-A	0.96	0.94
T-N	0.90	0.95
N-N	0.85	0.81
T-N ₂ -T	0.98	0.92
N ₄	0.95	0.94

^aDNA hairpins depicted in Figure 2. Comparison of these values reveals how well the CD spectrum of each modified hairpin agrees with that of the control hairpin at the two temperatures. For perfect agreement $r^2 = 1.0$.

DISCUSSION

We have performed a full analysis of the melting thermodynamics of DNA hairpins containing a 5-NI base or bases in the stem and loop regions. Both optical and DSC melting experiments provided evaluations of the transition thermodynamics of the

hairpins and a consistent rank order of their stabilities. However, as discussed below, the DSC and optical thermodynamic parameters, ΔH_{Cal} and ΔH_{vH} and ΔS_{Cal} and ΔS_{vH} , are in considerable disagreement.

The orders of the transition temperatures, T_m , and melting free energies of the hairpins obtained by both optical and DSC experiments agree exactly at N₄ > T-N₂-T > C > N-N > N-A > T-N. Hairpins containing a 5-NI base or bases in the stem of the duplex are destabilized up to 2.0 kcal/mol compared to the control hairpin, while hairpins containing two and four 5-NI bases in the loop region are more stable than the control by up to 1.0 kcal/mol. The origins of the added stability of the hairpins having 5-NI bases in the loop is not known, but it seems logical that if conventional Watson-Crick type base pairing between bases in the loop does not occur, then enhanced stacking interactions between the 5-NI bases in the loop and hydrophobic interactions with surrounding solvent could be a source of the observed higher stability. Since the 5-NI bases are more hydrophobic than the natural DNA bases, hydrophobic interactions between two or more contiguous 5-NI bases in the loop could likely increase hairpin stability. The proposition that hydrophobic interactions occur between 5-NI bases was raised by Loakes *et al.* (1). Self-association of consecutive (up to 21) 5-NI bases in a 64 base DNA template used for base recognition studies in PCR experiments resulted in the formation of a large hairpin type structure (1). It would be expected that self-association of the hydrophobic 5-NI bases would have a smaller destabilizing influence than instability from hydrophobic effects when the 5-NI bases are in the duplex and/or single strands.

Our DSC experiments provide no direct evidence for intermolecular self-association of the hairpins with 5-NI bases in the loops. DSC melting experiments were performed at strand concentrations up to 187 times higher than in the optical melting experiments. For modified hairpins containing more than one 5-NI base, $T_{m\text{Cal}}$ values are from 3 to 4°C higher than $T_{m\text{Opt}}$ values. Our data show that hairpins with the 5-NI bases in the loop are relatively more stable than hairpins with the 5-NI base or bases in the stem. This might be evidence for the presence of favorable intramolecular interactions between the bases in the loops that result in their increased stability. The increased stability could also arise from favorable intermolecular interactions in self-associated structures that form at the higher DNA concentrations at which DSC melting curves were measured. However, as shown in Figure 4, the DSC melting curves contain a single symmetric peak with no obvious evidence for aggregation. Interestingly, the hairpins with the 5-NI bases in the loop were even more stable than the control hairpin having a T₄ loop and no 5-NI bases. Melting studies of hairpins with the same duplex stem and X₄ loops (X = A, T, G or C) showed those with X = T were the most stable (7,9,13). When single-stranded DNA primers for sequencing were prepared with tails of 5-NI added to the 5'-end, only the primers with less than six 5-NI bases were functional. This is probably because the 5-NI tails can loop back upon themselves and self-pair (15), thus providing further evidence for favorable self-association of the 5-NI bases. Since the 5-NI base is approximately the same size as a natural base, the difference in entropy reduction associated with closing the hairpins with 5-NI bases in the loop versus a T₄ loop is probably not substantial enough to account for the observed increase in stability.

The CD spectra provide a different means of comparing the different hairpins. For the six hairpins the CD spectra are very similar, typical of right-handed B-DNA. Analysis by SVD of the CD spectra collected at 10 and 80°C, at which the strands reside in the fully duplex hairpin and denatured single-stranded form, respectively, reveals that the 5-NI bases have spectral features slightly different from the control in both the hairpin and denatured single-stranded states. This is especially evident in the spectra for hairpin N-N, in which the 5-NI bases are forced to be in relatively close contact. For this molecule, the CD spectra of both the duplex and single-stranded states differ the most from the control. If these spectral differences can be taken to be indicative of structural features, then these results suggest that subtle differences exist between the structures of the modified hairpins with 5-NI in the stems and the control hairpin. In contrast, the similarity between the CD spectra of the hairpins with the 5-NI bases in the loop region and the control suggests that if the 5-NI bases disrupt duplex and/or single-stranded structure of these molecules the disruption is not substantial enough to significantly affect the CD spectra, suggesting that if structural differences exist between the duplex and single-stranded states, they are very subtle. The CD spectroscopic data support the interpretations of the optical and DSC melting data.

Further comparison of the values of the optical and DSC parameters in Table 2 for all hairpins, including the control, shows that $\Delta H_{\text{Cal}} > \Delta H_{\text{vH}}$, $\Delta S_{\text{Cal}} > \Delta S_{\text{vH}}$ and $\Delta G_{293 \text{ Cal}} > \Delta G_{293 \text{ vH}}$. In the case of the control hairpin ΔH_{Cal} is 13% higher than ΔH_{vH} . This difference is slightly outside the limits of the collective experimental error (~7%) involved in determination of the optical and DSC parameters. The optical and DSC entropy values for the control, ΔS_{vH} and ΔS_{Cal} , are within 8% of one another. When these parameters are combined, the optical DSC free energies, $\Delta G_{293 \text{ vH}}$ and $\Delta G_{293 \text{ Cal}}$, differ by 42%. As mentioned above, these comparisons of thermodynamic parameters strongly suggest that the melting process of the control hairpin is not strictly two-state. As Table 2 further reveals, for the modified hairpins containing a 5-NI base or bases, differences between optical and DSC parameters are even greater. For these molecules the DSC parameters ΔH_{Cal} and ΔS_{Cal} are only 47–67% of their two-state optical values, ΔH_{vH} and ΔS_{vH} . Likewise, the DSC free energies, $\Delta G_{293 \text{ Cal}}$, are only 41–72% of their optical counterparts, $\Delta G_{293 \text{ vH}}$. In addition, enthalpy and entropy values determined from a two-state analysis of the DSC melting curves (not shown) were only 55–84% of the optical two-state parameters and 10–20% greater than the DSC values. Obviously, these differences are significantly outside the limits of experimental error and far greater than the differences between the optical and DSC parameters found for the control. If the lack of agreement between the ΔH_{Cal} and ΔH_{vH} values is due only to deviations from a two-state melting behavior (there is a significant population of partially melted intermediates during the melting transition) then it is remarkable that such short DNA hairpins would

display the observed deviations. *A priori* it would not be expected that such small hairpins would deviate significantly from two-state melting or at most deviate only slightly (as observed for the control hairpin). However, this is not consistent with the observed DSC parameters.

One plausible explanation for the observed relatively smaller values of ΔH_{Cal} and ΔS_{Cal} versus ΔH_{vH} and ΔS_{vH} in Table 2 and the relatively larger values of $\Delta \Delta H_{\text{Cal}}$ and $\Delta \Delta S_{\text{Cal}}$ versus $\Delta \Delta H_{\text{vH}}$ and $\Delta \Delta S_{\text{vH}}$ in Table 3 is suggested by the hydrophobic nature of the 5-NI base. It is possible that due to this greater hydrophobicity, exposure to aqueous environments results in significant solvent effects that perhaps include ordering of solvent water around the 5-NI base or bases. Such solvent effects have been commonly invoked to explain thermodynamic responses to the introduction of organic molecules into polar aqueous environments (15). If such solvent effects occur to a greater extent around the 5-NI bases in the melted single strand than in ordinary (unmodified) single strands, such as the melted control hairpin, then they might be expected to make an exothermic contribution with a positive enthalpy change and reduced entropy due to solvent ordering. If such solvent effects did not measurably perturb or otherwise disrupt base pair stacking, then they might not be detected in optical melting experiments. They could also manifest in the evaluated thermodynamics by introducing configurational constraints of the duplex and melted hairpin states. The net result of these solvent effects would be an overall increase (less negative values) of ΔH_{Cal} and ΔS_{Cal} measured by DSC.

REFERENCES

- Loakes, D., Hill, F., Brown, D.M. and Salisbury, S.A. (1997) *J. Mol. Biol.*, **270**, 426–435.
- Bergstrom, D.E., Zhang, P., Toma, P.H., Andrews, P.C. and Nichols, R. (1995) *J. Am. Chem. Soc.*, **117**, 1201–1209.
- Loakes, D. and Brown, D.M. (1994) *Nucleic Acids Res.*, **22**, 4039–4043.
- Papageorgiou, C. and Tamm, C. (1987) *Helv. Chim. Acta*, **70**, 138–141.
- Ohtsuka, E., Matsuki, S., Ikehara, M., Takahashi, Y. and Matsubara, K. (1985) *J. Biol. Chem.*, **260**, 2605–2608.
- Lin, P.K. and Brown, D.M. (1992) *Nucleic Acids Res.*, **20**, 5149–5152.
- Vallone, P.V., Paner, T.M., Hilario, J., Lane, M.J., Faldasz, B.D. and Benight, A.S. (1999) *Biopolymers*, **50**, 425–442.
- Cantor, C.R., Warshaw, M.M. and Shapiro, H. (1970) *Biopolymers*, **9**, 1059–1077.
- Paner, T.M., Amaratunga, M., Doktycz, M.J. and Benight, A.S. (1990) *Biopolymers*, **29**, 1715–1734.
- Marky, L.A. and Breslauer, K.J. (1987) *Biopolymers*, **26**, 1601–1620.
- Amaratunga, M., Pancoska, P., Paner, T.M. and Benight, A.S. (1990) *Nucleic Acids Res.*, **18**, 577–582.
- Cantor, C.R. and Schimmel, P.R. (1980) *Biophysical Chemistry*, Part II: *The Behavior of Biological Macromolecules*. W.H. Freeman and Co., New York, NY, p. 1175.
- Senior, M.M., Jones, R.A. and Breslauer, K.J. (1988) *Proc. Natl Acad. Sci. USA*, **85**, 6242–6246.
- Ball, S., Reeve, M.A., Robinson, P.S., Hill, F., Brown, D.M. and Loakes, D. (1998) *Nucleic Acids Res.*, **26**, 5225–5227.
- Cantor, C.R. and Schimmel, P.R. (1980) *Biophysical Chemistry*, Part I: *The Conformation of Biological Macromolecules*. W.H. Freeman and Co., New York, NY, pp. 279–288.